ICE SHIELD FOR OFFSHORE STRUCTURES

Mohamed A. Hamed (1), Amgad Hussein (1), and Hesham Marzouk (2)

(1) Department of Civil Engineering, Memorial University of Newfoundland, St John's, Canada.

(2) Department of Civil Engineering, Ryerson University, Ontario, Canada.

Abstract:

This investigation focuses on Ultra-High Performance Fibre Reinforced (UHP-FRC) concrete as a possible material for ice shield for offshore applications. A composite flexural element was constructed from two layers of concrete. The top layer was made with UHP-FRC with a compressive strength of 170 MPa and thickness 50 mm. The bottom layer is a High Performance Concrete (HPC) with a compressive strength of 85 MPa and thickness of 180 mm. The two layers were connected with shear keys and T-headed studs to transfer the interface shear between the layers. The experimental program investigated the structural behaviour of the composite specimen. The results revealed that there was an increase in the ultimate flexural capacity when compared to the non-composite beams. The T-headed studs were capable of transferring the interface shear up to the failure of the composite specimen. On the other hand, the use of shear keys did not enable the full transfer of the shear stresses in the plastic region. The equation proposed by Loov and Patnaik (8) gave the best predictions of the interface shear stress when compared the experimental results.

Résumé:

Cette recherche porte sur l'application potentielle du béton fibré à ultra-hautes performances (BFUP) pour des coques de protection contre les glaces de structures à la mer. Un élément mixte travaillant en flexion a été réalisé en deux couches : celle du dessus en BFUP de résistance en compression 170 MPa et d'épaisseur 50 mm, celle du dessous en béton à hautes performances (BHP) de résistance en compression 85 MPa et d'épaisseur 180 mm, les deux couches étant connectées grâce à des indentations et des goujons en T pour transférer le cisaillement d'interface. Le programme d'essais a exploré le comportement structurel de cet élément mixte. Les résultats ont mis en évidence une amélioration de la capacité ultime en flexion par rapport aux éléments non-mixtes. Les goujons se sont avérés capables de transférer le cisaillement d'interface jusqu'à la rupture du corps d'épreuve mixte, alors que les indentations n'ont pas permis un transfert complet des contraintes de cisaillement dans la zone plastique. L'équation proposée par Loov et Patnaik (8) a donné les meilleures prévisions de la contrainte d'interface par rapport aux résultats expérimentaux.

1. INTRODUCTION

Gravity based structures showed great success in the North Atlantic Ocean with its harsh and aggressive environment. Ice shields are used to protect offshore platforms in cold harsh environment from ice friction during the winter season. Prince Edward Island Bridge used steel ice shields on the first bridge piers, whereas on later piers, the ice shields were cast in high strength concrete. Sakhalin 2 development also used steel ice shield to protect the structure. The light house in the Baltic Sea used concrete as an ice shield but the concrete was badly damage from the ice abrasion [1].

Ultra high performance Fibre Reinforced Concrete (UHP-FRC) is one of the recent advances in material applications that have substantial growth in the field of the structural engineering. UHP-FRC was first developed during the mid-1990's with a compressive strength more than 160 MPa and a flexural strength greater than 30 MPa [2]. UHP-FRC has advantageous properties such as low permeability, corrosion resistance, abrasion resistance, and high durability in aggressive environment in addition to its high tensile strength, flexibility, and toughness [3].

UHP-FRC is a suitable material to construct ice shields for offshore platforms. The shield could act in a composite manner with the high performance concrete that is normally used to build the platform. One of the important aspects to be considered in the design of composite elements is the horizontal shear transfer between the two layers of concrete. The horizontal shear stress is usually transferred through the friction of concrete-on-concrete, adhesion, and reinforcement between the two layers. For a composite section to develop the full flexural capacity (Figure 1(a)), the interface bond between the layers should always remain intact. Figure 1 (b) shows the flow of horizontal shear between the two layers of concrete. If the composite element is incapable of transferring the developed shear stresses between the two layers, slippage will occur and the horizontal shear stress is no longer transferred between the two layers as shown in Figures 1(c) and (d).

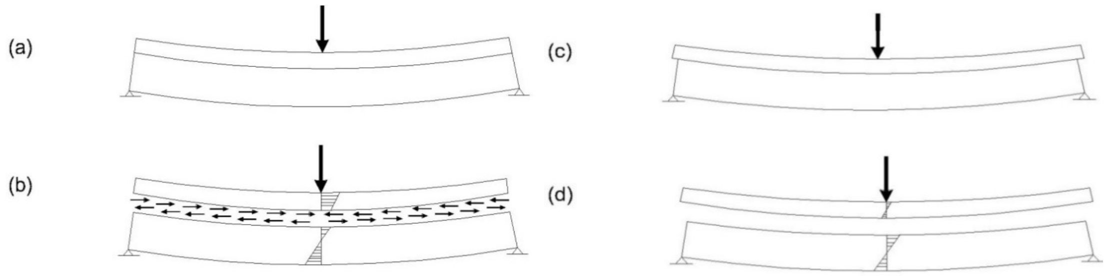

Figure 1: Simply supported beam: (a) composite beam, (b) shear stresses at the interface, (c) non-composite beam, and (d) horizontal shear slip. Adapted from reference [4]

Overlays are used in the pre-cast industry, on top of concrete bridge decks, and in rehabilitation and strengthening of the concrete structures. Design equations to calculate the shear stresses are given in codes such as AASHTO [5], ACI [6], and Eurocode 2 [7]. Some researchers stated that the code equations may not be accurate in estimating the horizontal shear stress along the interface and proposed alternative design equations [8-9].

In recent studies, UHP-FRC was investigated as a possible material to be used in the pre-cast industry [10]. Recent experimental investigations on overlays and composite members can be found in references [10-12]. A large body of work on the use of UHPFRC in the repair and rehabilitation of bridges and structures was carried out at EPFL [13-17]. The extensive research program showed that perfect bond between UHPFRC and concrete could be obtained by preparing the concrete substrate surface by high pressure water jetting or by sand blasting.

The current investigation aims to study the flexural behavior of composite flexural elements made with UHP-FRC. The main objective is to examine the effect of different types of interface connections. The experimental results are also compared with the predictions of different code and researchers' proposed equations to calculate the horizontal shear stress along the interface.

2. EXPERIMENTAL PROGRAM

2.1 Material details

Two types of concrete were used to construct the composite test specimen. The top layer was cast using UHP-FRC and the bottom one was cast using high performance concrete (HPC). The UHP-FRC was designed to achieve a compressive strength of 170 MPa after 28 days. Short straight steel fibres were used in the mixture and the fibre volume content was 2 %. The HPC bottom layer was designed to reach a compressive strength of 85 MPa on the day of testing. Cold drawn steel wire fibres with hooked ends were used. The fibres were 35 mm in diameter and had an aspect ratio of 65 and tensile strength of 1345 MPa. The fibre volume content was 0.75 %.

2.2 Details of test specimen

Three specimens were cast and tested to failure. All specimens had a length of 1950 mm and a width of 300 mm. The reference specimen (HSC-00-50) was non-composite and it had a thickness of 230 mm as shown in Figure 2(a). The second (SK-195-50) and third (THS-195-50) specimens were composite ones as shown in Figure 2(b and c). The composite specimens were constructed with a top layer of 50 mm-thick UHP-FRC that contained 10M steel mesh in the middle of the layer. The bottom layer was HPC with a thickness of 180 mm and it was reinforced with 2-10M top and 4-15M bottom bars. The clear cover was 20 mm and the reinforcement grade was 400 MPa. The shear reinforcement used was 10M stirrups every 200 mm. In addition to the shear keys in specimen SK-195-50, which had a dimension of 75 mm wide, 75 mm long, and 25 mm high, T-headed shear studs and concrete were used to fill the shear keys in specimen THS-195-50 to improve the shear transfer between the two layers of concrete. Details of the test specimen are shown in Table 1. The composite specimens were cast in two stages. The top UHP-FRC layer was cast first. Formwork was placed around the top layer and the bottom layer was then cast.

Table 1: Specimen details

Name	UH Thickness (mm)	HSC Thickness (mm)	Total Thickness (mm)	Shear Connections	Spacing (mm)
HSC-00-50	0	230	230	N/A	N/A
SK-195-50	50	180	230	Shear Key	195
THS-195-50	50	180	230	T-Headed Studs	195

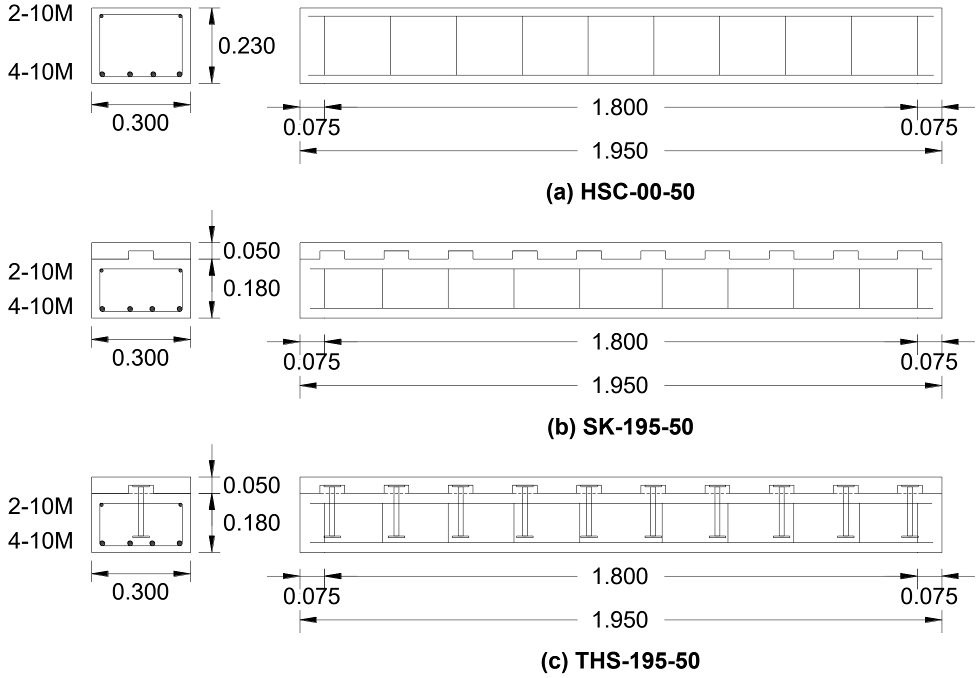

Figure 2: Details of test specimen (all dimensions are in meters)

2.3 Test set-up & procedure

A photograph of the test set-up and instrumentation is depicted in Figure 3. All specimens were simply supported and loaded with four-point loading. The loading was applied using a 670 kN servo-hydraulic MTS actuator in displacement control. The load was then divided into two point loads. The distance between the two loads was 130 mm and the span between the two supports was 1850 mm. The applied load was measured using a load cell. The deflection at mid-span and quarter-spans were measured using LVDTS. The concrete and steel strains were measures using electrical strain gauges. The relative slippage at the interface between the top and bottom layers was measured using displacement transducers.

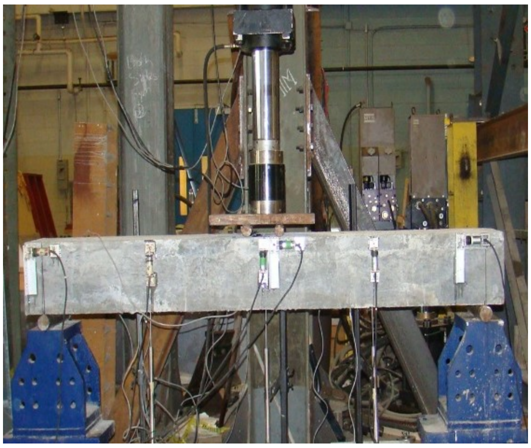

Figure 3: Test set-up

Each specimen was preloaded to approximately 15 kN to minimize the settlement of the beam. During a test, the load was applied in increments of approximately 8.8 kN. At each load increment, the beam was inspected and the cracks were monitored and mapped until the specimen failed. The applied load, deflections, and strains from the different sensors were recorded using a high-speed data acquisition system. The data was monitored by a personnel computer using LABVIEW program and stored on the hard disk of the computer. The frequency of the data sampling was 2.0.

3. RESULTS AND ANALYSIS

Figure 4 shows the load versus mid-span deflection for all test specimens. By inspecting the figure, it can be noticed that all specimen appeared to behave in a similar fashion. Up to the first cracking load, all specimens experienced a linear elastic behaviour. The slope of that line is the un-cracked stiffness of the specimens. As the load was increased further, the load deflection curves remained almost linear but with a slightly lower slope. At this stage, the cracked stiffness of the specimens was reduced due to the formation of cracks. With further application of the load, the load-deflection curves deviated from linearity until a plastic load-deflection state was attained. All specimens had a decreasing load-deflection slope until failure occurred. The use of shear keys or T-headed reinforcement did not have any significant impact on the un-cracked and cracked stiffness of the specimen.

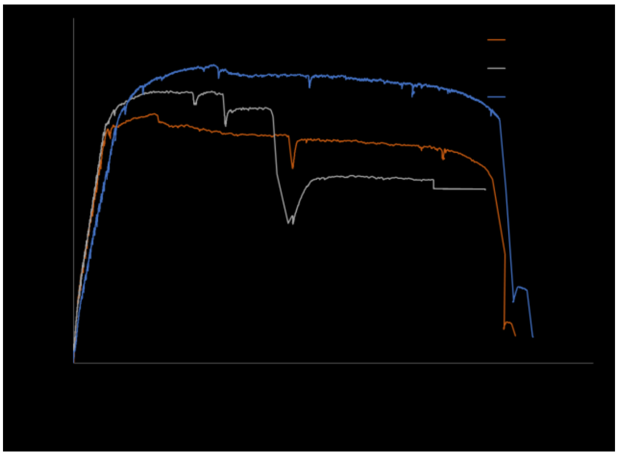

Figure 4: Load vs. mid-span deflection

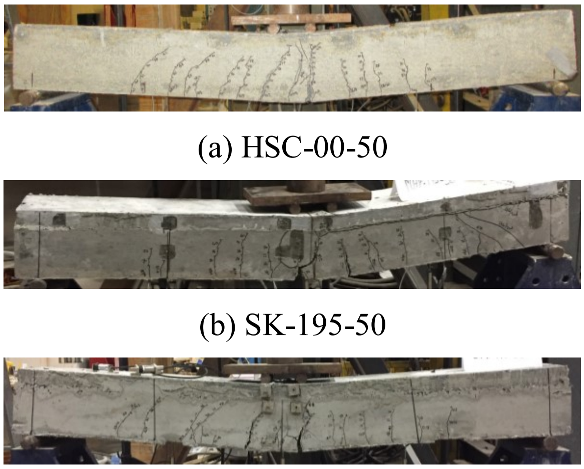

(a) HSC-00-50

(b) SK-195-50

(c) THS-195-50

Figure 5: Crack patterns at failure

The first crack occurred in the middle of the specimen at the tension side of HPC layer as expected. As the load was increased, the cracks started to propagate in a typical flexural fashion. For specimen SK-195-50 with shear keys, the cracks did not penetrate into the top UHP-FRC layer. On the other hand, the cracks propagated into the top UHP-FRC layer in specimen THS-195-50. Figure 5 shows a picture of the crack patterns near failure. The non-composite reference specimen HSC-00-50 reached a peak load of 101 kN. The load gradually decreased until the specimen failed at a load of 92 kN. Specimen SK-195-50 attained a peak load of 110 kN and failed at 104 kN.

A sudden drop in the load occurred in the plastic region. Slippage at the interface between the two layers of concrete was observed as some of the shear keys failed and a noise was heard. The specimen was no longer acting as a composite element, and the horizontal shear stress was no longer transferred between the two layers and each acted separately. The specimen had an increase in its flexural capacity of 9 % from the non-composite specimen. Specimen THS-195-50, with T-headed studs, had the highest peak load of 122 kN and it failed at a load of 97 kN. The specimen did not experience any slippage at the interface between the two layers. However, a crack at the interface was observed. The sample acted as a true composite section and the studs were capable of transferring the interface shear until the specimen failed. The sample had a 21 % in flexural capacity over the non-composite reference specimen. A summary of test results is given in Table 2.

Table 2: Summary of Test Results

Specimen	First Crack (kN)	Peak Load (kN)	Failure Load (kN)
HSC-00-50	26.6	101.0	92.2
SK-195-50	22.2	110.4	104.5
THS-195-50	26.7	122.3	97.5

4. HORIZONTAL SHEAR STRESS

Five equations were used to evaluate the interface shear stress and compare the results with experimental results. The five equations used were from the AASHTO [5], ACI [6], Loov and Patnaik [8], Khan and Mitchell [9], and Eurocode 2 [7].

AASHTO [5] $$V_n = cA_{cv} + \mu\left[A_v f_y + P_c\right] \tag{1}$$

ACI [6] $$V_n = \lambda\left[1.8 + 0.6\frac{A_v f_y}{b_v s}\right] b_v d \tag{2}$$

Khan and Mitchell [9] $$v_n = 0.05f_c^{'} + 1.4\frac{A_v f_y}{b_v s} \leq 0.2f_c^{'} \tag{3}$$

Loov & Patnaik [8] $$v_n = K\sqrt{\left(0.1 + \frac{A_v f_y}{b_v s}\right) f_c^{'}} \tag{4}$$

Eurocode 2 [7] $$V_n = cf_{cd}A_{cv} + \mu(A_v f_y + P_c) \tag{5}$$

where, v_u is the horizontal shear stress in the interface of the composite element; V_u is the shear strength on the composite element; b_v is the width of the composite element; d is the depth of the composite element; f_c' or f_{cd} is the weaker concrete compressive strength; f_y is the yield stress of transverse reinforcement; A_{cv} is the area of concrete in which the interface shear stress in being transferred; A_v is the area of interface shear reinforcement crossing the shear plane within A_{cv}; s is the spacing between interface shear reinforcement; μ is the friction factor; c is the cohesion factor; and P_c is the permanent net compressive force normal to the shear plane. The experimental interface shear stress was obtained as follows:

$$v_n = \frac{V_u}{b_v d} \tag{6}$$

Table 3 contains the experimental interface shear stress along with the interface shear stress capacities calculated using the Equations 1 through 6. The interface shear stress for specimen SK-195-50 was 1.9 MPa. This value is greater than the predicted values by the different equations for a specimen that does not contain shear key.

Table 3: Experimental and predicted values of interface shear stresses, MPa

Specimen	Experimental	AASHTO	ACI	Loov & Patnaik	Kahn & Mitchell	Eurocode 2
Assuming no shear key or T-headed studs		0.71	1.8	0.87	4.5	0.5
THS-195-50	2.1	1.44	2.7	2.28	6.4	1.88

From Table 3, it is apparent that Loov and Patnaik expression [8] was the best indicator to estimate to the interface shear stress for the specimen with T-headed studs. On the other hand, AASHTO [5] gave a very low estimate of the interface shear stress and Eurocode 2 [7] was higher than the AASHTO [5] but incorrect estimate of the interface shear stress. ACI [6] was slightly unconservative. Kahn and Mitchell equation [9] gave a very high estimate for the interface shear stress.

5. CONCLUSIONS

The current experimental investigation was conducted to investigate the behaviour of UHPC/HPC composite specimens. Two types of interface connections were investigated; namely shear keys and T-headed shear connectors. The following conclusions can be drawn from the results.

– The shear keys or T-headed reinforcement did not have any significant impact on the un-cracked and cracked stiffness of the specimen.
– The composite specimens exhibited an increase in the ultimate flexural capacity when compared to the non-composite reference specimen. The composite element with T-headed studs showed the highest enhancement in the ultimate flexural capacity.
– The test results revealed that the T-headed studs were capable of transferring the interface shear up to the failure of the composite specimen. On the other hand, the use of shear keys did not enable the full transfer of the shear stresses in the plastic region.
– Loov and Patnaik [8] equation (4) was the best indicator of the interface shear stress when compared the experimental results.

REFERENCES

[1] *Concrete Structures for Oil and Gas Fields: In Hostile Marine Environments*. Lausanne, Switzerland: International Federation for Structural Concrete (fib), 2009. Print.

[2] Nematollahi, B., R, R. S. M., Jaafar, M. S., & Voo, Y. L. (2012). A review on ultra high performance “ductile” concrete (UHPdC) technology. *International Journal of Civil and Structural Engineering*, *2*(3), 1003–1018. http://doi.org/10.6088/ijcser.00202030026

[3] Wille, K., Naaman, A. E., El-Tawil, S., & Parra-Montesinos, G. J. (2011). Ultra-high performance concrete and fiber reinforced concrete: achieving strength and ductility without heat curing. *Materials and Structures*, *45*(3), 309–324. http://doi.org/10.1617/s11527-011-9767-0

[4] Kovach, J. D., & Naito, C. (2008). Horizontal Shear Capacity of Composite Concrete Beams without Interface Ties, ATLSS REPORT NO. 08-05, Leigh University, 236 p.

[5] AASHTO LRFD Bridge design Specifications. (2012). *AASHTO LRFD Bridge design specifications*. Washington, DC: American Association of State Highway and Transportation Officials.
[6] ACI Committee 318. (2014). *ACI 318M-14. Building Code Requirements for Structural Concrete*. Farmington Hills, Mich., American Concrete Institute.
[7] CEN European Committee for Standardization, "Eurocode 2: Design of Concrete Structures – Part 1-1: General Rules and Rules for Buildings (EN 1992-1-1)," Brussels, Belgium, 2004, 225 pp.
[8] Loov, Robert E., Patnaik, A. K. (1994). Horizontal Shear Strength of Composite Concrete Beams with a Rough Interface. *PCI Journal*, *39*, 48–67.
[9] Kahn, L. F., & Mitchell, A. D. (2002). Shear friction tests with high-strength concrete. ACI Structural Journal, 99(1), 98–103.
[10] Crane, C. K., & Kahn, L. F. (2012). *Interface shear capacity of small UHPC/HPC composite T-beams*. Ultra-High Performance Concrete and Nanotechnology in Construction, Proceedings of Hipermat 2012 3rd International Symposium on UHPC and Nanotechnology for High Performance Construction Materials, Kassel University press.
[11] Nes, L. G., & Øverli, J. A. (2015). Structural behaviour of layered beams with fibre-reinforced LWAC and normal density concrete. *Materials and Structures*, *49*(1–2), 689–703. http://doi.org/10.1617/s11527-015-0530-9
[12] Baran, E. (2015). Effects of cast-in-place concrete topping on flexural response of precast concrete hollow-core slabs. *Engineering Structures*, *98*, 109–117. http://doi.org/10.1016/j.engstruct.2015.04.017
[13] Brühwiler, E. (2016, July). "Structural UHPFRC": Welcome to the post-concrete era!. In Proceedings, Keynote Lecture, 1st US-UHPC Symposium Des Moines USA.
[14] Bastien Masse, M. (2015). "Structural Behavior of R-UHPFRC-RC Composite Slabs". Doctoral thesis No. 6841, École Polytechnique Fédérale de Lausanne (EPFL), Switzerland.
[15] Habel, K. (2004). Structural behaviour of elements combining ultra-high performance fibre reinforced concretes (UHPFRC) and reinforced concrete. Doctoral thesis No. 3036, École Polytechnique Fédérale de Lausanne (EPFL), Switzerland.
[16] Makita, T. (2014). Fatigue behaviour of UHPFRC and R-UHPFRC-RC composite members. Doctoral thesis No. 6068, École Polytechnique Fédérale de Lausanne (EPFL), Switzerland.
[17] Oesterlee C., (2010) "Structural response of reinforced UHPFRC and RC composite members", Doctoral thesis No. 4848, École Polytechnique Fédérale de Lausanne (EPFL), Switzerland.